

Bulletin of Scientific Contribution GEOLOGY

Fakultas Teknik Geologi UNIVERSITAS PADJADJARAN

homepage: http://jurnal.unpad.ac.id/bsc p-ISSN: 1693-4873; e-ISSN: 2541-514X



GEOTHERMAL POTENTIAL IDENTIFICATION BASED ON REMOTE SENSING ANALYSIS IN IJEN GEOTHERMAL FIELD, EAST JAVA

Ridwan Nur Fauzi¹, Aton Patonah², Santi Dwi Pratiwi², Kazuyo Hirose³, Pradnya Paramarta Raditya Rendra²

¹Undergraduate program, Faculty of Geological Engineering, Universitas Padjadjaran.

²Universitas Padjadjaran, Faculty of Geological Engineering, Jl. Raya Bandung Sumedang km 21, Jatinangor, Indonesia.

³Japan Space Systems, 3-5-8 Shibakoen, Minato-ku, Tokyo, Japan

ABSTRAK

Panasbumi merupakan sumberdaya energi terbarukan yang dimanfaatkan untuk berbagai kebutuhan baik sebagai energi panas untuk skala lokal hingga produksi listrik dalam skala industri. Pencarian sumberdaya panasbumi merupakan hal yang sulit dan memakan banyak biaya sehingga dibutuhkan suatu metode survey yang dapat memudahkan tahap eksplorasi panasbumi pada cakupan area yang luas. Metode penginderaan jauh dapat menjadi alat yang memadai untuk memandu penyelidikan area prospek panasbumi melalui penjabaran peta potensi sumberdaya hidrotermal pada tingkat zona potensi yang menguntungkan untuk dieksploitasi. Tujuan dari penelitian ini adalah untuk mengidentifikasi area yang mendukung untuk dilakukan eksplorasi dan eksploitasi panasbumi di kawasan Pegunungan Ijen, Jawa Timur. Metode yang digunakan meliputi pemrosesan citra sensor OLI (Operational Land Imager) dan TIRS (Thermal Infrared Sensor) dari satelit Landsat-8 untuk mendapatkan sebaran zona alterasi hidrotermal dan anomali suhu permukaan. Identifikasi zona permeabel berdasarkan densitas rekahan pada daerah penelitian juga dilakukan dengan analisis data Digital Elevation Model (DEM) untuk mendapatkan fitur topografi daerah penelitian. Hasil penelitian menunjukan adanya korelasi antar parameter yang digunakan pada beberapa daerah yang kemudian di interpretasi sebagai zona prospek panasbumi. Zona prospek sedang hingga tinggi ditemukan berasosiasi dengan sebagian besar keberadaan manifestasi panasbumi yang diketahui.

Kata Kunci: Zona prospek panasbumi, penginderaan jauh, zona alterasi, anomali suhu permukaan, Densitas patahan dan rekahan.

ABSTRACT

Geothermal is a renewable energy resource that is used for various needs, both as heat energy on a local scale to electricity production on an industrial scale. The search for geothermal resources is difficult and costly, thus a survey method is needed that can facilitate the geothermal exploration stage in a large area coverage. Remote sensing methods can be an adequate tool to quide investigations of geothermal prospect areas through the elaboration of potential hydrothermal resource maps at the level of profitable potential zones for exploitation. The purpose of this study is to identify areas that support geothermal exploration and exploitation in the Ijen Mountains area, East Java. The method used includes processing OLI (Operational Land Imager) and TIRS (Thermal Infrared Sensor) sensor images from the Landsat-8 satellite to obtain the distribution of hydrothermal alteration zones and surface temperature anomalies. Identification of permeable zones based on fracture density in the study area was also carried out by analyzing Digital Elevation Model (DEM) data to obtain the topographical features of the study area. The results of the study show that there is a correlation between the parameters used in several areas which are then interpreted as geothermal prospect zones. The moderate to high prospect zone was found to be associated with most of the known presence of geothermal manifestations.

Keywords: Geothermal prospect zone, remote sensing, alteration zone, surface temperature anomaly, fault fracture density.

INTRODUCTION

The Ijen Mountains are one of the locations suspected of having potential geothermal resources that can be developed. The results of geophysical, geochemical and geological analysis indicate that the estimated geothermal reserves of the Ijen Mountains up to 133 MWe, of which 110 MWe are in Mount Ijen, while 23 MWe are in the vicinity of Mount Rauna (Cahyono, 2019). Geothermal can be identified from potential manifestations that appear on the surface. manifestations Surface are all forms, appearances, symptoms, and earthly activities on the surface that indicate the possibility of geothermal potential in the area (Sumatoro, 2015). Remote sensing technology has high observation accuracy and relatively low cost for broad unity, thus providing the possibility to integrate the level of accuracy and efficiency in the supply of geothermal data and information. This study aims to determine geothermal potential zones in the Blawan-Ijen area based on analysis of alteration zones, surface temperature, and lineament density through remote sensing observation methods. The stratigraphy of the

Ijen mountain complex is composed of Old Ijen Volcanic Rocks (Qpvi), Raung Volcanic Rocks (Qhvr), Young Ijen Volcanic Rocks (Qhvi), Merapi Volcanic Rocks (Qvm), Lake Blawan Deposits (Qbs) and Reef Limestones (QI). Old Ijen Volcano rocks (Qpvi) are Pleistocene in age and are composed of breccia, tuff pumice breccia and basalt lava. Raung Volcanic Rocks (Qhvr) are Pleistocene to Holocene in age and are composed of volcanic breccias and tuff. Young Ijen Volcanic Rocks (Qhvi) is composed of breccia tuff and basaltic lava. Merapi Volcanic Rock (Qvm) is composed of breccia alternating with sandy tuff and lava-inserted tuff. Lake Blawan Deposits (Qbs) is composed of tuffaceous clay. Reef Limestone (QI) is composed of limestone with conglomerate and tuff inserts. The four rock units are Holocene in age (Sidarto et al. 1993) (Figure 1). The appearance of the geological structure in the Ijen Caldera can be observed from rivers and/or series of volcanoes. In general, the deformation that occurs in the Ijen Caldera can be caused by the reactivation of the magma chamber, tectonic activity, or by a combination of both.

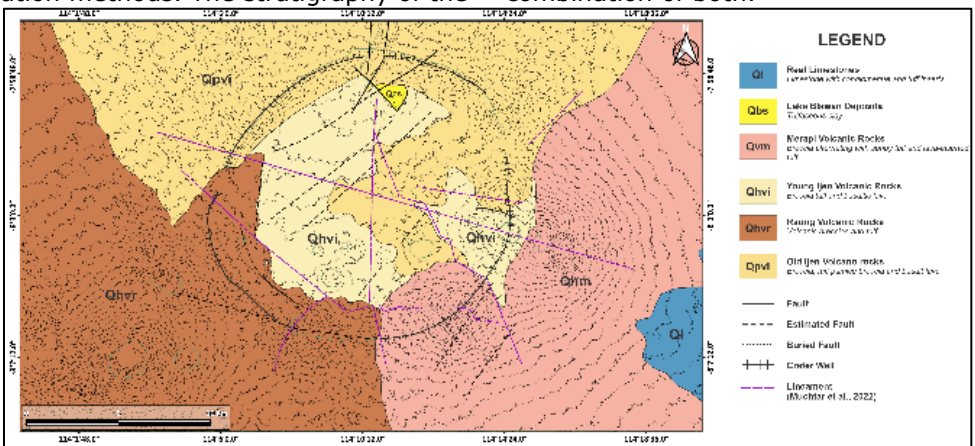


Figure 1. Regional Geological Map of Mount Ijen Area (modified from Sidarto et al., 1993).

METHOD Satellite Data

The method used in this study includes observations of satellite imagery and digital elevation models (DEM). Landsat 8 images were acquired from USGS EarthExplorer which is then analyzed to obtain the distribution of alteration minerals and earth's surface temperature. DEM data was obtained from DEMNAS which is a combination of IFSAR, TERRASAR-X and ALOS PALSAR with a resolution of 0.27-arcsecond or ~8.1 m. DEM provides better observations of the morphology of the earth and can provide better observations of lineaments as an indication of the influence of geological structures.

Alteration Zones

The initial stage in processing satellite images includes atmospheric corrections carried out FLAASH (Fast Line-of-sight Atmospheric Analysis of Spectral Hypercubes) module. In the processing stage, the image is processed using band ratio and PCA (Principal Component Analysis) method. The technique of band rationing enhances as well as improves the compositional information of a satellite image while at the same time suppressing information that may not be useful (Ombiro et al., 2021). The bands used in mineral mapping are related to the reflectance spectra and the positions of the mineral absorption bands or mineral assemblages (Figure 2).

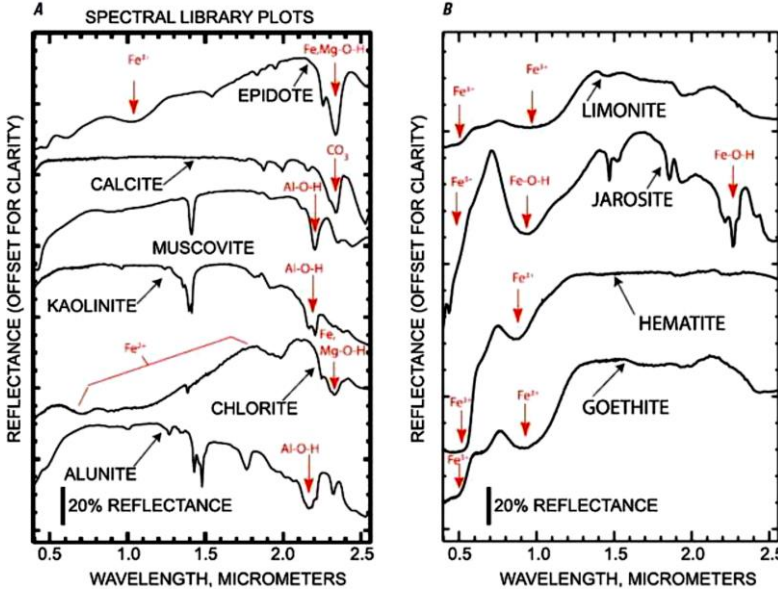


Figure 2. Laboratory spectra of alunite, chlorite, kaolinite, muscovite, calcite, and epidote. (B) Laboratory spectra of limonite, jarosite, hematite, and goethite (Clark et al., 1993).

Several band ratios can provide information about hydrothermal alteration minerals and lithology units. The distribution of alteration minerals is mapped through the following band ratios:

Band ratio 4/2 - iron oxides

Band ratio 6/7 - hydroxyl bearing rocks

Band ratio 7/5 - clay minerals

Band ratio 6/5 - ferrous minerals

A composite of band ratios is arranged to separate the altered rocks from other surface objects. The composite used follows Sabin's ratio (4/2, 6/7, and 6/5 as RGB) and band ratio 4/2, 6/7, and 5 as RGB (Pour et. al., 2015).

PCA (Principal Component Analysis) method is used to reduce the effect of vegetation on the image through a spectral unmixing technique. The PCA method is enhancement and refinement technique that transforms the initial correlation data into several uncorrelated variables known as Principal Components (PC). The PC is chosen based on the magnitude of the band's influence on each PC observed from the eigenvector value where the value away from zero means the band had most significance on the PC. Bands 2, 4, 5 and 6 and bands 2, 5, 6 and 7 of Landsat 8 were subject to PCA analysis. This is done to highlight areas associated with iron oxides and hydroxyl minerals from vegetation.

Land Surface Temperature

LST was derived using the emissivity of the Earth's surface (LSE), the gloss temperature and the difference in emissivity between the LSE of the TIR bands 10 and 11 (Morabit et al., 2021). LST depends on the distribution of temperature on the earth's surface and the

of emissivity the spectral channel measurement (Becker and Li, 1995). Band 4 and 5 of Landsat 8 image can detect the presence of vegetation and soil moisture to calculate NDVI while Band 10 and 11 are thermal bands. LST values can be calculated as follows:

Digital Number (DN) conversion to Top of Atmospheric Radiance

$$L_{\lambda} = M_L \cdot Q_{cal} + A_L \tag{1}$$

Where:

 L_{λ} = Spectral radiance (W/m2)

 M_L = Band-specific multiplicative rescaling factor

 Q_{cal} = Digital number corresponds to band 10 and band 11

 A_{I} = Band-specific additive rescaling factor Band Radiance conversion to Brightness Temperature (TB)

$$BT = \frac{K_2}{\ln(\frac{K_1}{L_1} + 1)} - 273.15 \tag{2}$$

Where:

BT = Brightness temperature (K)

 L_{λ} = TOA radiance

 K_1 = Spectral radian calibration constant

= Absolute temperature constant

Calculating Normalized Difference Vegetation Index (NDVI)

$$NDVI = \frac{\rho_{nir} - \rho_{red}}{\rho_{nir} + \rho_{red}}$$
 (3)

Where:

nir = Band 5

red = Band 4

Vegetation Fraction (PV) calculation

$$Pv = \frac{NDVI - NDVI_{min}}{NDVI_{max} + NDVI_{min}}$$
(4)

Calculating Emissivity (E)

$$e = m \cdot Pv + n \tag{5}$$

Where:

e = Land surface emissivity

m =Surface emissivity standard deviation constant (0.4)

n = The emissivity value of vegetation minus (0.986)

Satellite temperature conversion to Land Surface Temperature (LST)

$$T = TB/[1 + \left(\lambda \cdot \frac{TB}{c2}\right) \cdot ln(e)] \tag{6}$$

Where:

 λ = wavelength of emitted radiance (Band 10 = 10.8 µm; Band 11 = 12 µm)

$$c2 = h * c/s = 1.4388 * 10^{-2} m K = 14388$$
 umK

The images used correspond to a Landsat 8 TIRS of 18th September 2017, 29th October 2018, and 25th August 2020. These images were selected for dominant surface coverage on those dates and least affected by atmospheric phenomenon such as clouds or smoke. Table 1 shows the values defined for three highest temperature ranges of satellite thermal images.

Table 1. Satellite temperature classification. Three ranges of maximum temperature were defined and classified qualitatively.

No	Temperature 1	Qualitative Classification		
1	23	27	Low	
2	27	32	Medium	
3	32	40	High	

Fault and Fracture Density

Lineament feature extraction was carried out in PCI Geomatica with input parameters using the parameters proposed by Thannoun (2013) for LINE modular (Table 2). The creation of a slope direction shading map can automatically direct the position of the slope identical to the illumination angle on the shaded relief, the result of this process is an RGB image that represents the slope direction in a gradational way. Lineament extraction

refers to the topographic changes and shapes observed in the slope direction shading map.

Table 2. The input value for each parameter of the LINE algorithm (Tannoun R.G., 2013).

RADI (Filter Radius)	5
GTHR (Gradient threshold)	75
LTHR (Length threshold)	10
FTHR (Line fitting error threshold)	2
ATHR (Angular difference threshold)	20
DTHR (Linking distance threshold)	1

The lineament density map is made with the help of the Geographic Information System (GIS) application, by converting density values into a contour map which then analyzed to determine the permeable zone in the study area.

Geothermal Potential Zones

The prospect of the Ijen geothermal area was obtained by making a spatial superposition of the three index maps. The objective was to identify the areas where the highest index values were superimposed. That means, high satellite temperature, high structural density and occurrence of altered zones.

RESULT AND DISCUSSION Distribution of Alteration Minerals

In this study, the ratio of Landsat 8 OLI band 4 to band 2 was used to highlight areas with abundant presence of iron oxide-bearing minerals, the presence of minerals is indicated by red pixels. The ratio of band 6 to band 5 shows the distribution of ferrous minerals shown in green pixels. Clay minerals, such as illite, kaolinite, and montmorillonite are shown in the ratio of band 7 to band 5 as yellow pixels. The ratio of band 6 to band 7 shows the distribution of alunite and hydrothermal clay minerals as blue pixels (Figure 3).

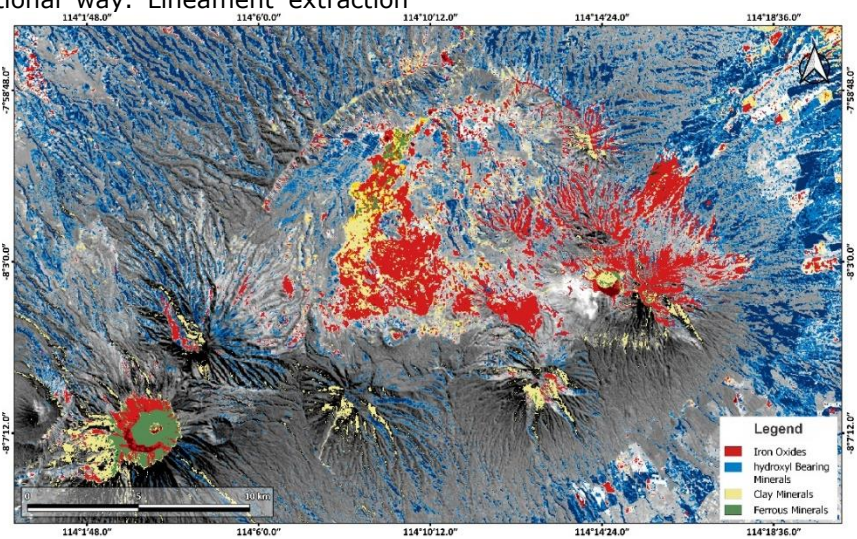


Figure 3. Band ratio image shows the distribution of iron oxide, hydroxyl bearing minerals, clay minerals, and ferrous minerals.

Band ratios 7/5 and 6/7 which show the distribution of clay minerals and alunite has a wider distribution to the distal zone of the crater. While the ratio of the bands 4/2 and 6/5 shows the concentration of ferrous and iron oxide minerals in the proximal zone of the volcano and the middle part of the Old Ijen Crater.

Composites arranged on this band ratio can separate outcrops of altered rock from

unaltered rock and highlight areas where concentrations of these minerals occur. Images created using Sabin's ratio (4/2, 6/7 and 6/5 as RGB) are shown for mapping lithology and hydrothermal alteration zones (Figure 4A). For the same purpose another RGB Composite is formed with bands 4/2, 6/7, and 5 (Figure 4B).

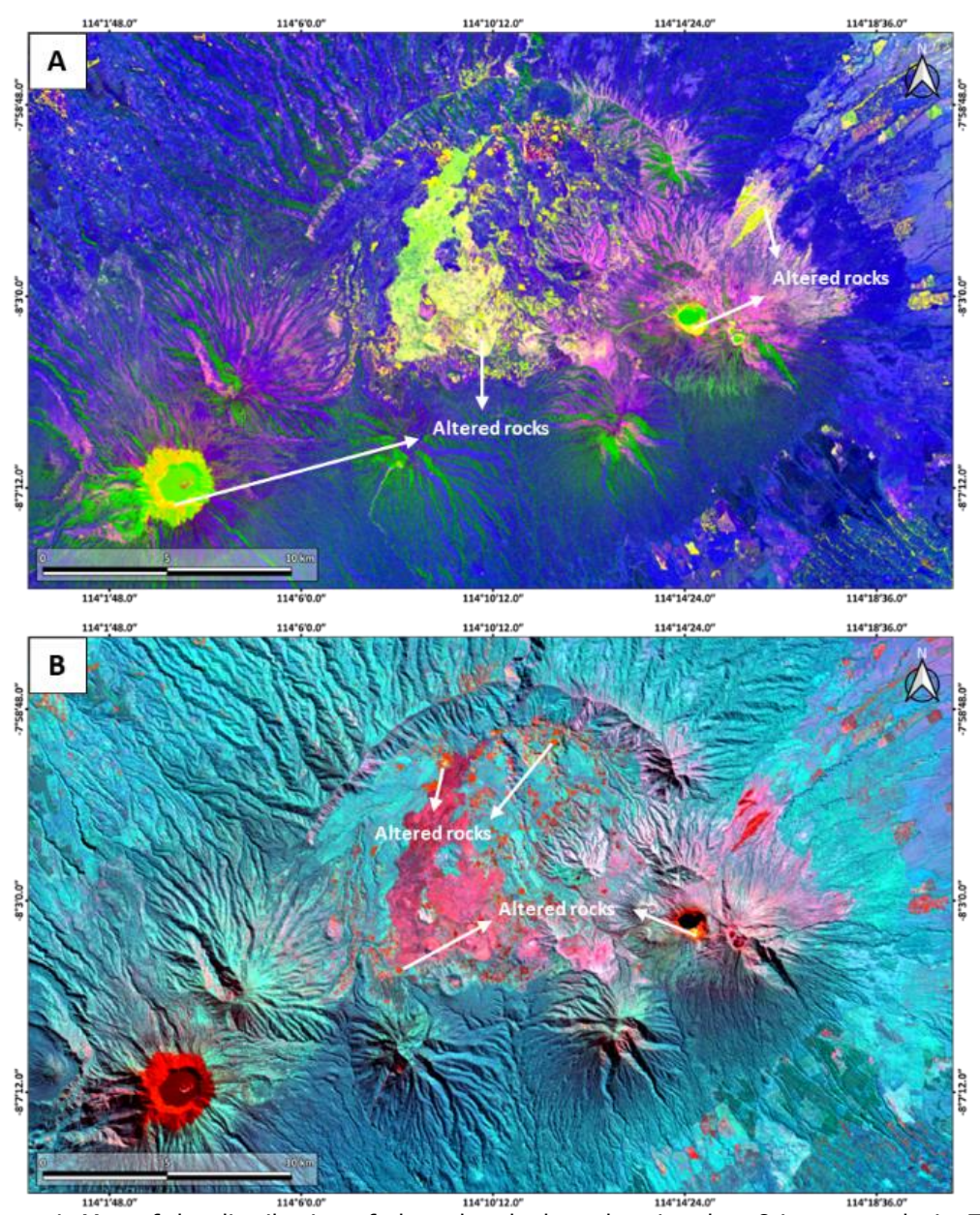


Figure 4. Map of the distribution of altered rocks based on Landsat 8 image analysis. The map shows the distribution of altered rocks as yellow pixels in Sabin's ratio (A), and orange pixels in band ratio 4/2, 6/7, and 5 (B).

Altered rocks are shown as yellow in sabin's ratio while in composite bands 4/2, 6/7, and 5 the alteration zone is shown as orange pixels. The findings on both composites show the position of the alteration zone which is interrelated, while some of the others show

an alteration zone that is not visible in the other composites.

Iron oxide is a constituent in the alteration zone associated with sulfide deposits and can be identified by band 4/band 2 ratio (Sabins, 1999; Poormirzaee & Oskouei, 2010, Pour &

Hashim, 2015). Meanwhile, hydroxyl bearing minerals are alteration products with the widest distribution and are associated with a diversity of clays and sheet silicates, which contain Al-OH and Mg-OH groups and hydroxides in the alteration zone (Poormirzaee & Oskouei, 2010).

The PCA method allows identification of the Principal Component (PC) which contains more spectral information of the Landsat 8 bands. The magnitude of the eigenvector loadings in each PC corresponds to the spectral properties of surface materials such as rock, vegetation, and soil (Crosta and Moore, 1989). Table 3 displays the loadings of the Landsat 8 PCA results bands 2, 4, 5, and 6 for iron oxide minerals.

Table 3. Eigenvector and eigenvalues of the Principal Component in Landsat 8 bands 2, 4, 5, and 6 for iron oxide minerals.

	PC1	PC2	PC3	PC4
BAND 2	0.03222	0.17246	0.63965	0.74838
BAND 4	0.04748	0.37145	0.65975	-0.65154
BAND 5	0.92256	-0.37003	0.10136	-0.04108
BAND 6	0.38157	0.83388	-0.38119	0.11723
EIGENVALUES	779325.98919	88748.36216	7126.63152	1001.05019
PERCENT OF	88.9436	10.1288	0.8134	0.1142
EIGENVALUES	88.9430	10.1288	0.8134	
ACCUMULATIVE OF	88.9436	99.0724	99.8858	100
EIGENVALUES				

PC4 shows the eigenvector loadings is positive for band 2 (0.74838) and negative for band 4 (-0.65154). These two bands have a greater loading in PC analysis, pixels with abundant presence of iron oxide minerals can be identified as bright pixels (Figure 5).

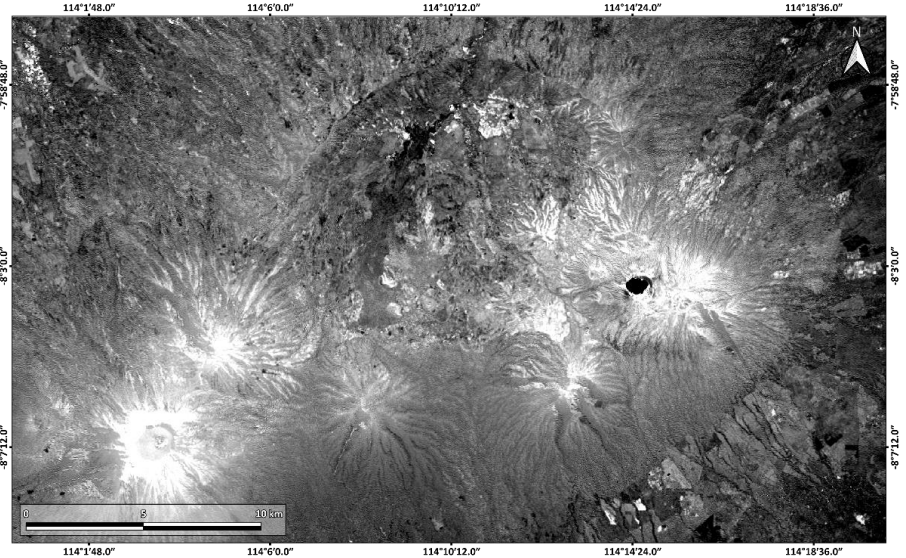


Figure 5. The Principal Component of Landsat 8 data for iron oxide minerals (PC4) is shown as bright pixels.

By the same method, the distribution of the hydroxyl bearing minerals for PCA bands 2, 5, 6 and 7 is shown in Figure 6.



Figure 6. Principal Components from Landsat 8 data for hydroxyl carrier minerals (PC4) are shown as bright pixels.

Images with pixels showing anomalous concentrations of hydroxyl and iron oxide bearing minerals as the brightest pixels were created by combining images showing concentrations of hydroxyl and iron oxide with the Crosta method. This new image is combined with the other two RGB composites (iron oxide, iron oxide & hydroxyl, hydroxyl). This process produces colored composites

where the dark pixels are alteration zones which are areas where the rock contains concentrations of iron (iron-stained) and hydrothermal clay minerals; cyan to blue color is an area where the rock is more argillized (minerals are converted to form clay) than contain iron; the orange to red zones are zones where rocks contain more iron than clay minerals (Figure 7).

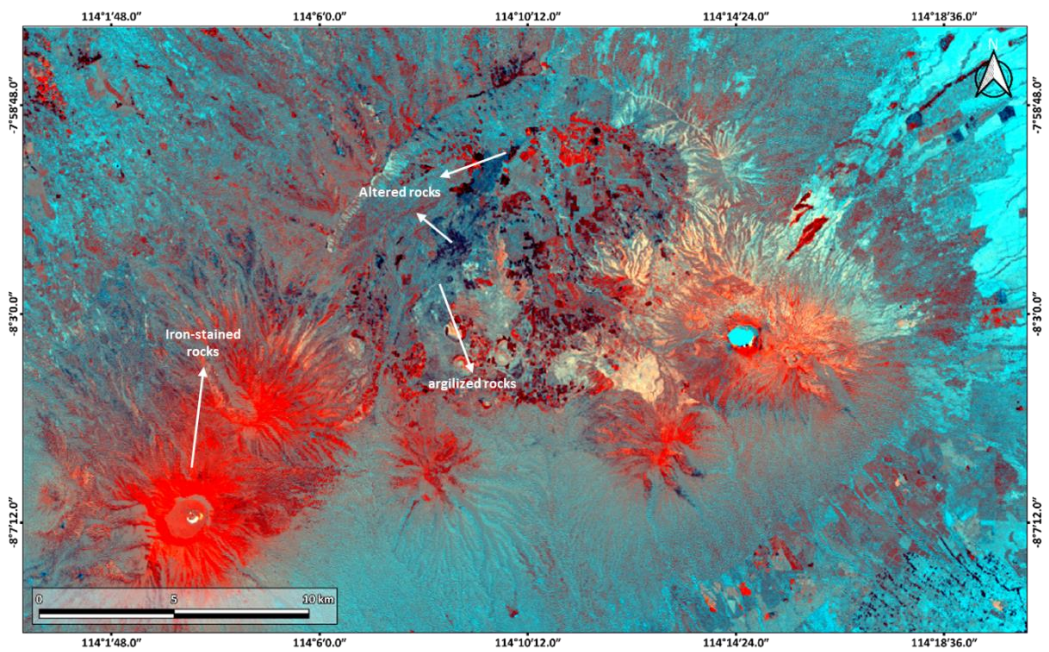
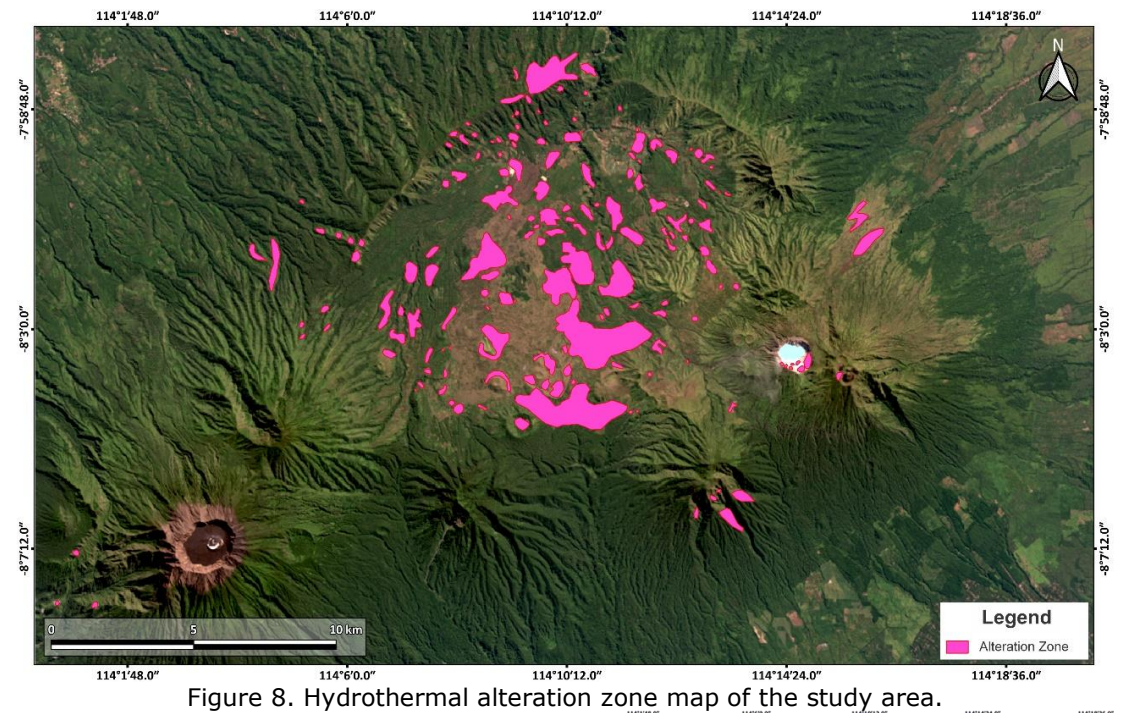


Figure 7. The RGB composite of the resulting images of PC4 hydroxyl, hydroxyl and iron oxide, and iron oxide. This composite image shows areas of hydrothermal alteration as dark pixels.

Figure 8 shows the spatial distribution of hydrothermally altered rocks identified based on the results from band ratios and PCA images (Figs 4A; 4B; and 7). This method highlights areas where mineral

concentrations or mineral assemblages from alteration processes such as iron-bearing minerals and hydroxyl-bearing minerals occur, separating altered and unaltered rocks.



Land surface temperature

Land Surface Temperature (LST) is the average appearance of the temperature on the surface. The higher the ground surface temperature of an area, the higher the potential for geothermal energy in that area (Zhang, 2012). The results of the surface temperature analysis of Landsat 8 imagery on September 18th, 2017, October 29th, 2018, and August 25th, 2020, show temperature anomalies in images that are similar in shape and magnitude (Figure 9).

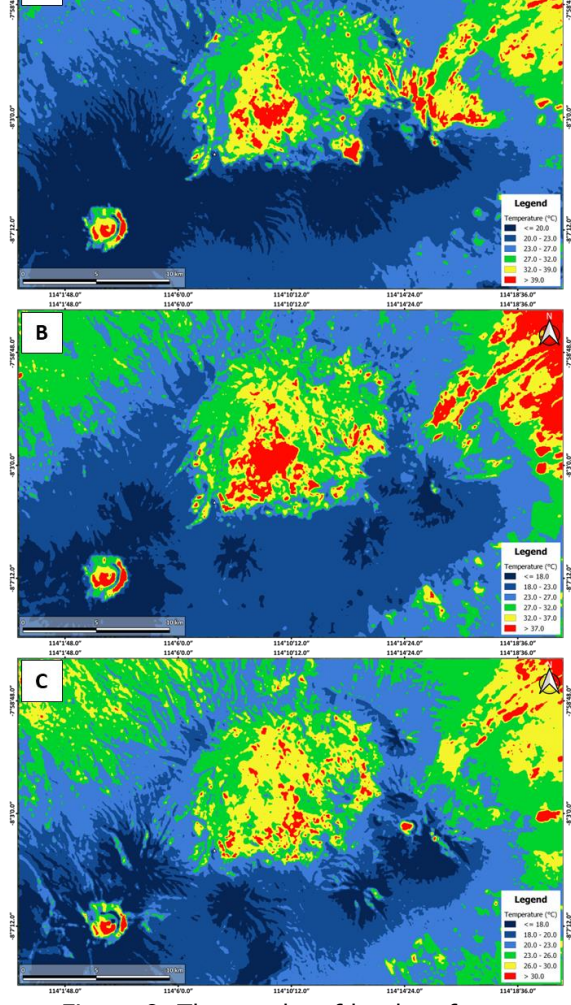


Figure 9. The results of land surface temperature image processing on September

18th, 2017 (A), October 29th, 2018 (B), and August 25th, 2020 (C).

The results of surface temperature analysis from the three images are then classified based on table 1. Then an overlay is performed to obtain an index map of surface temperature anomalies in the study area (Figure 10).

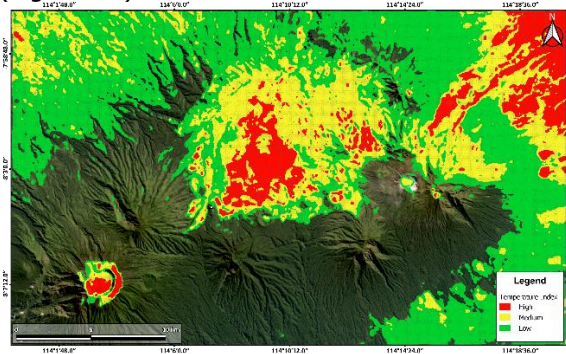


Figure 10. Surface temperature index map of the study area.

Fault and Fracture Density

Based on fracture density map. It is interpreted that the study area can be divided into high, medium and low-density areas. Areas with high fracture density occupy the northern part and part of the east, west and south directions of Old Ijen Crater, it can also be observed that the areas with high density are associated with the circular structure of the walls of Old Ijen Crater and the lineaments that cut through the center of the crater in a north - south direction. Areas with medium fracture density occupy the central, western, and southeastern parts of the study area. Medium fracture density in the center of the crater can be caused by deposits of intracaldera volcanoes in the form of lava that covers secondary structures and porosity in the study area. Areas with low fracture densitv occupy the southwestern southeastern parts of the study area (Fig.

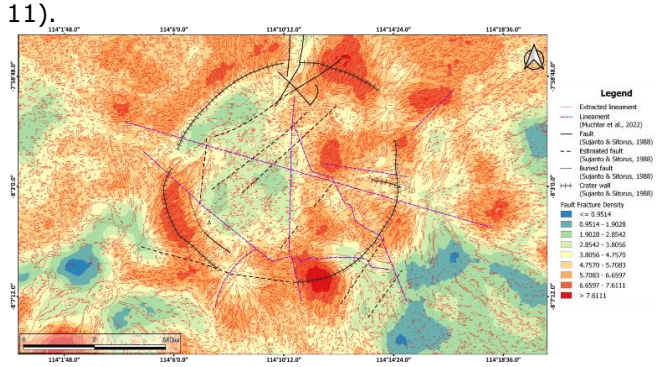


Figure 11. Fault and fracture density map of study area.

Geothermal Prospect Zone

The geothermal prospect map is created based on fault and fracture density maps (FFD), surface temperature index (LST) maps, and distribution of alteration zones in the study area to identify areas where geothermal manifestations can be found. This map was compiled based on data obtained from Landsat 8 and DEM imagery as well as several geological assumptions, namely: Faults and fractures can act as pathways for geothermal fluids to emerge to the surface High surface temperatures may be associated with the presence of subsurface heat sources Alteration rock is an indication

hydrothermal activity that changes the composition of the rock

Based on the information obtained from analysis of Landsat 8 and DEM imagery, a correlation between lithology and structural information in the study area can be compiled to determine geothermal exploration targets with a higher probability of finding geothermal prospects (Figure 12)

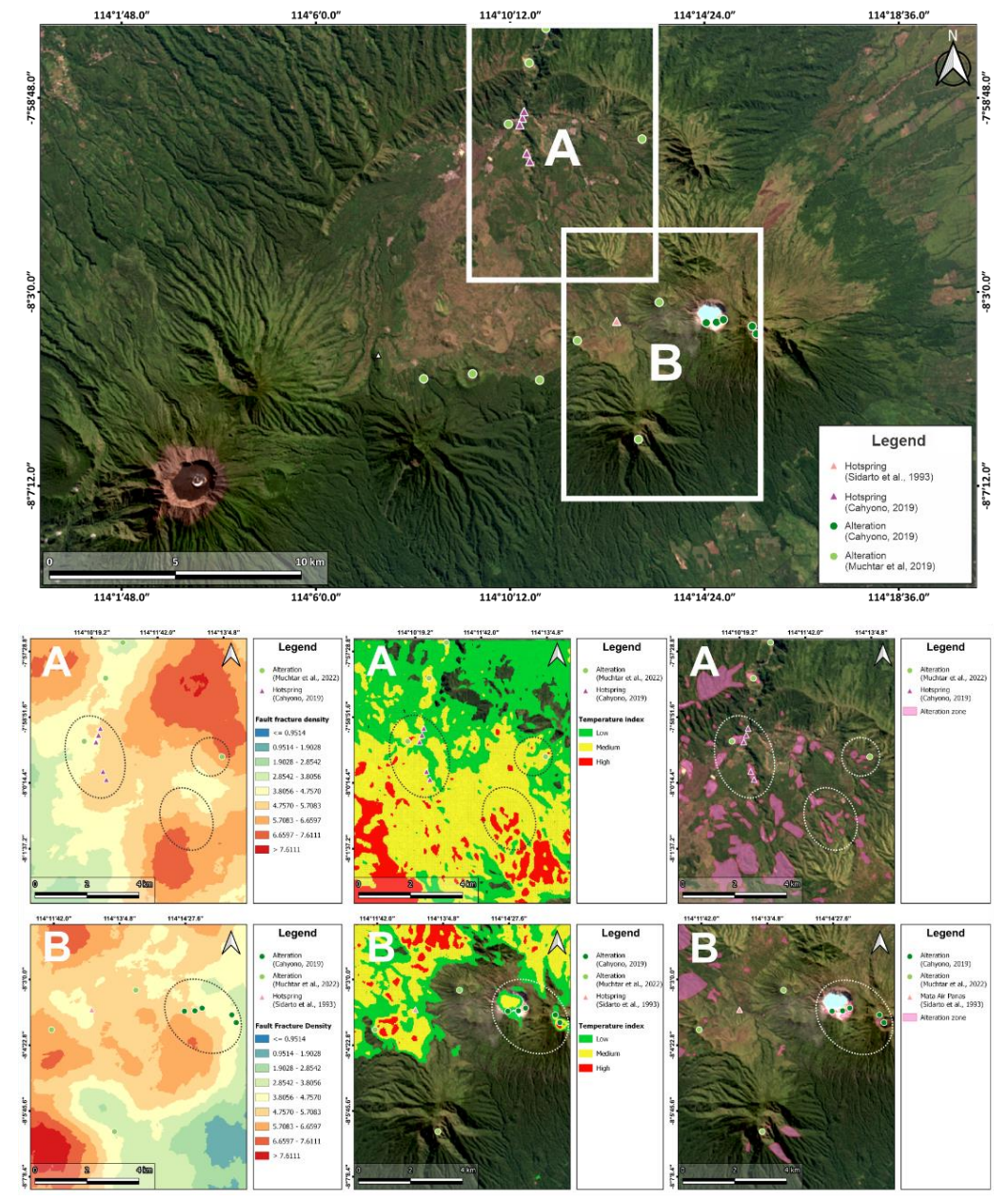


Figure 12. Correlation between fracture density map, surface temperature, and distribution of alteration zone in research area (A) Outflow zone of geothermal system; (B) Upflow zone of the geothermal system in the study area.

Information obtained from remote sensing observations is then presented in a geothermal prospect map to facilitate the

identification of new exploration targets with the possibility of finding geothermal manifestations in the study area (Figure 13).

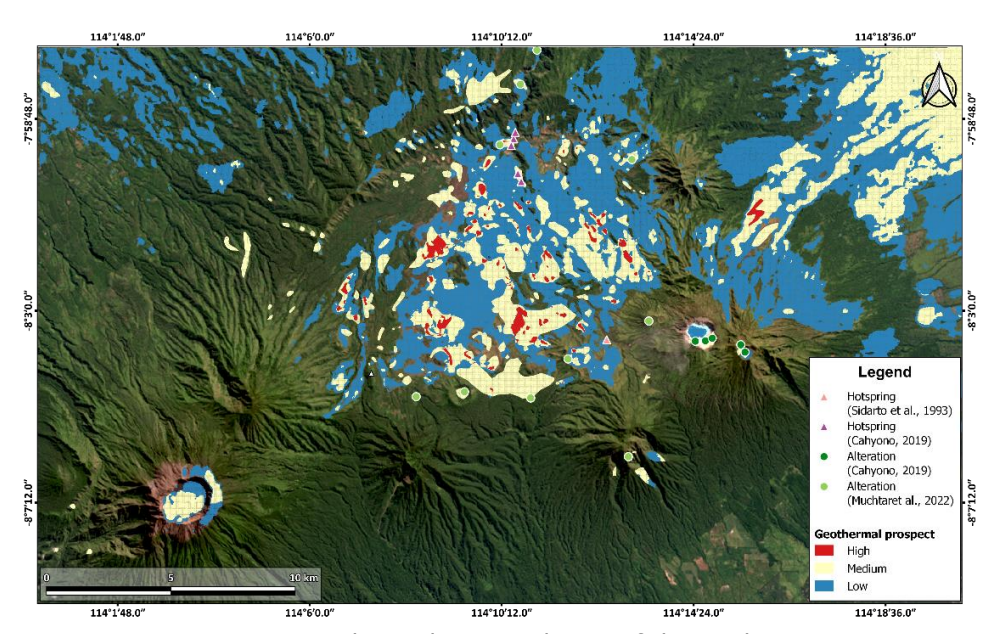


Figure 13. Geothermal potential map of the study area.

Exploration targets are stated in 3 categories. namely low, medium, and high based on the probability of findina geothermal manifestations in the area. The distribution of this geothermal potential zone tends to head north from the Ijen Mountains complex. This is also supported by the presence of bicarbonate-sulfate hot springs in the Blawan area which indicates the possibility of the outflow zone heading north in the direction of the hot springs (Daud et al., 2016). So it can also be assumed that the upflow zone is likely to be around the Iien crater and Merapi mountain to the southeast where the elevation is higher than other areas. The geological conditions which are dominated by lava in the study area can cover geological so that structures permeable observations based on remote sensing methods can be difficult things to do.

CONCLUSION

The existence of an alteration zone indicated by the appearance of iron oxide minerals and hydroxyl bearing minerals is not too extensive because it is covered by young volcanic deposits. The distribution of alteration zones can generally be found in the interior of the Old Ijen Crater. High surface temperatures in permeable areas may be an indication of hydrothermal fluids being influenced by geological structures, while low levels of permeability with hiah temperature anomalies may be influenced by the characteristics and permeability of rock porosity. Analysis of Landsat 8 and DEM shows potential geothermal imagery exploration areas for further investigation. The results show a low to high geothermal exploration potential area where most of the known geothermal manifestation observation points are associated with medium to high potential areas. The distribution of geothermal potential in the study area tends towards the north where the northern part of the Ijen mountains is interpreted as an outflow zone which is characterized by the presence of geothermal manifestations in the form of hot springs.

REFERENCES

Ali, A., and Pour, A., 2014. Lithological mapping and hydrothermal alteration using Landsat 8 data: a case study in ariab mining district, red sea hills, Sudan. *International Journal of Basic and Applied Sciences*, 3(3), 199–208.

Cahyono, B.E., 2019. Analisis Sebaran Potensi dan Manifestasi Panasbumi Pegunungan Ijen Berdasarkan Suhu Permukaan dan Geomorfologi.

Clark, R.N., Swayze, G.A., Wise, R., Livo, E., Hoefen, T., Kokaly, R. and Sutley, S.J., 2007. USGS digital spectral library splib06a: U.S. Geological Survey, Digital Data Series 231.

Crosta, A.P. and Rabelo, A., 1993. Assessing of Landsat TM for hydrothermal alteration mapping in central western Brazil . Proceedings of Ninth Thematic conference geologic remote sensing Pasadinea, p. 1053-61, California, USA.

Daud, Y., Nuqramadha, W.A., Fahmi, F.Z., Pratama, S.A., Rahman, K.R., and Subroto, W., 2017. Discovering "Hidden" Geothermal Reservoir in Blawan-Ijen Geothermal Area (Indonesia) Using 3-D Inversion of MT Data.

Daud, Y., Rosid, M. S., Fahmi, F., Yunus, F. M., and Muflihendri, R., 2018.

- Identification of geothermal prospect zone in Ijen Caldera (East Java) using geomagnetic method and landsat data analysis. Faculty of Mathematics and Natural Sciences (FMIPA), Universitas Indonesia. DOI: 10.1063/1.5064267
- Goetz, A., 2009. Three decades of hyperspectral remote sensing of the Earth: A personal view. *Remote Sensing of Environment*, 113, pp. 5-16.
- Goetz, A.F.H., Rowan, L.C. and Kingston, M.J., 1982. Mineral identification from orbit: initial results from the Shuttle Multispectral Infrared Radiometer. *Science*, 218, pp. 1020-1031.
- Han, T. and Nelson, J., 2015. Mapping hydrothermally altered rocks with Landsat 8 imagery: A case study in the KSM and Snow field zones, northwestern British Columbia. In: Geological Fieldwork 2014, British Columbia Ministry of Energy and Mines, British Columbia Geological Survey Paper, 2015-1, pp.103-112.
- Mateus, R., 2015. Mapping hydrothermal gold mineralization using Landsat 8 data. A case of study in Chaves license, Portugal. Departamento de Geociências, Ambiente e Ordenamento do Território
- Muchtar, A., M Manurung, Z. K., Suparman, Y., and Ishak Jumarang, M., 2022. Identifikasi Zona Reservoir Panas Bumi Gunung Ijen Jawa Timur Berdasarkan Pemodelan 2 Dimensi Anomali Geomagnetik Identification of Geothermal Reservoir Zone at Mount Ijen East Java Based on 2 Dimensional Modeling of Geomagnetic Anomalies. 12(1), 92–97.
- Ombiro, S.O., Olatunji, A.S., Mathu, E.M. & Ajayi, T.R. 2021. Application of remote sensing in mapping hydrothermally altered zones in a highly vegetative area A case study of Lolgorien, Narok County, Kenya. Indian Journal of Science and Technology 14(9): 810-825.https://doi.org/10.17485/IJST/v14i9.
- Pour, A. and Hashim, M., 2015. Hydrothermal alteration mapping from Landsat-8 data, Sar Chesmeh copper mining district, south-eastern Islamic Republic of Iran. Journal of Taibah University for Science, 9, 155-166.
- Raehanayati, Rachmansyah, A. and Maryanto, S. 2013. Studi Potensi Energi Geothermal Blawan-Ijen, Jawa Timur Berdasarkan Metode Gravity
- Sabins, F.F., 1999. Remote sensing for mineral exploration. Ore Geology Reviews 14, 157–183.
- Sidarto, Suwarti, T., and Sudana, D., 1993. Peta Geologi Lembar Banyuwangi, Jawa. Pusat Penelitian dan Pengembangan Geologi, Bandung.

- Van der Meer, D. F., 2004. Analysis of spectral absorption features in hyperspectral imagery. International Journal of Applied Earth Observation and Geoinformation, 5, 55 68.
- Zoheir, B., El-Wahed, M.A., Pour, A.B. and Abdelnasser, A., 2019. Orogenic Gold in Transpression and Transtension Zones: Field and Remote Sensing Studies of theBarramiya–Mueilha Sector, Egypt. Remote Sensing. 11(18):2122–2122.